Designing tomorrow's snow park jump

Article *in* Sports Engineering · March 2012

DOI: 10.1007/s12283-012-0083-x

CITATIONS
21

READS
310

3 authors, including:

James Mcneil
Colorado School of Mines
55 PUBLICATIONS **1,282** CITATIONS
SEE PROFILE

Mont Hubbard
University of California, Davis
171 PUBLICATIONS **2,194** CITATIONS
SEE PROFILE

Sports Eng (2012) 15:1–20
DOI 10.1007/s12283-012-0083-x

ORIGINAL ARTICLE

Designing tomorrow's snow park jump

James A. McNeil · Mont Hubbard · Andrew D. Swedberg

Published online: 31 January 2012

Abstract Recent epidemiological studies of injuries at ski resorts have found that snow park jumps pose a significantly greater risk for certain classes of injury to resort patrons than other normal skiing activities. Today, most recreational jumps are built by skilled groomers without an engineering design process, but the Snow Skiing Committee (F-27) of the American Society for Testing and Materials is considering the inclusion of recreational jumps in their purview which may lead to a greater role for engineering jump designs in the US in the future. Similar efforts are underway in Europe as well. The purpose of this work is to review the current state of the science of snow park jumps, describe the jump design process, and outline the role that modelling will play in designing tomorrow's snow park jumps.

1 Introduction

The last two decades have witnessed a dramatic evolution in the skiing industry worldwide. The number of participants on snowboards has increased and now approaches parity with skiers [1]. Based on data from the National Sporting Goods Association, of 11.2 million snow-slope participants in 2008, 5.3M skied only, 4.7M snowboarded only, and 1.2M did both. Because the snowboarding population is younger and demands more access to the acrobatic aspects of sliding than previously, ski resorts instituted and continue to experiment with snow terrain parks which include jumps and other airborne features. Epidemiological studies of injuries at ski resorts have found that snow park jumps pose a significantly greater risk for certain classes of injury to resort patrons than other skiing activities [2–5]. In particular, due to increases in flight maneuvers and associated landings, a corresponding increase in the frequency and severity of head, neck and upper-extremity injuries has been documented [2].

In a report widely publicized by the National Ski Areas Association (NSAA), Shealy et al. [6] noted that over the period from 1990 to the present when overall snow terrain park use has risen, overall injury rates have actually fallen. Yet, all studies that focus on actual terrain park injuries show that terrain parks do indeed present a special hazard to riders. The Shealy finding is most likely due to improved ski equipment and an aging, and therefore more cautious, demographic patron profile over the period covered in his study. Early research recognized that snowboard injury patterns differed from those of skiers [7], and that snowboard injury rates could be as much as six times higher than those of skiers [8]. The snowboard injury rate was discovered to have doubled between 1990 and 2000 from 3.37 to 6.97 per 1,000 participant days [9]. In addition, jumping was found early to be the most important cause of injury [8]. An increased risk of head injury at terrain parks as compared to ski runs continued through the end of the last decade [10]. A recent study of snowboard injury rates specifically in terrain parks found

J. A. McNeil (✉)
Department of Physics, Colorado School of Mines, Golden, CO 80401, USA
e-mail: jamcneil@mines.edu

M. Hubbard
Department of Mechanical and Aerospace Engineering, University of California, Davis, CA 95616, USA
e-mail: mhubbard@ucdavis.edu

A. D. Swedberg
Department of Mathematics, U.S. Military Academy, West Point, NY 10996, USA
e-mail: Andrew.Swedberg@usma.edu

that the risk of injury on jumps was highest of all terrain park features [3]. Another study comparing ski and snowboard injuries inside and outside terrain parks found that the percentage of spine and head injuries inside the terrain park was double that outside [4]. The principal hazards may be succinctly summarized as landing "hard" and/or landing upside down.

Many snow-related head, neck and back injuries are extremely serious. A succinct summary provided by Meyers and Misra [11] states: "spinal cord injuries (SCIs) are among the worst ski outcomes." A broad review of SCI epidemiological trends by Jackson et al. [12] found an increase in SCI caused by snow (as opposed to water) skiing, and that snow skiing (presumably including snowboarding) had replaced football as the second leading cause of SCI in the US. Ackery et al. [13] published a review of 24 articles between 1990 and 2004 from 10 countries and found evidence of an increasing incidence of traumatic brain injury and SCI in alpine skiing and snowboarding worldwide. They noted that this increase coincided with "development and acceptance of acrobatic and high-speed activities on the mountain".

By as early as the end of the 1990s, Tarazi et al. had found that the incidence of SCI in snowboarders was four times that in skiers and that jumping was the primary cause of injury (77% of snowboarder SCIs occurred from jumping) [1]. In a review by Seino et al. [14] of six cases of traumatic paraplegia SCIs resulting from snowboard accidents at a single institution over 3 years, researchers found that they occurred to young men between the ages of 23 and 25, and that the primary fracture mechanism was a backward fall from an intentional jump.

Although the above published studies are compelling, today it is still difficult to get a precise snapshot of overall terrain park injury statistics nation- or worldwide. In the US, although the NSAA collects skiing and snowboarding injury data, these data are not made publicly available.

These most serious SCIs (resulting in paraplegia or quadriplegia) exact a very large cost on society. That they happen uniformly to young people and are permanently debilitating means that there is an enormous economic and social cost (see [15, 16]). One would hope that these large costs would lead to a more careful and scientific approach to the design and fabrication of those terrain park features primarily involved, but this has not been the case.

Although terrain parks have improved in many ways over the years, the quality of the end product varies widely from resort to resort. There do exist creditable training programs, such as "Cutter's Camp" [17], that are intended to increase the knowledge and skill level of the groomers. These have helped considerably, but space in these courses is limited so such training is by no means universal. In addition, rider education efforts such as Burton's "Smart Style" have been beneficial. Yet adoption of quantifiable engineering design of terrain parks has been resisted. At present, in the US at least, terrain park jumps are typically fabricated at the individual resorts using little or no quantitative analysis or engineering design by staff with no formal training in engineering analysis of the designs.

The reluctance of ski resorts to adopt an engineering design approach may be traced to their risk management strategy. As gleaned from the waiver forms attached to lift pass agreements and recent presentations by ski industry defense lawyers, one apparent component of the legal strategy in the US is to assert that the responsibility for safety resides with the patrons. Aside from minimum diligence related to roping, signage, lifts, rental shop operations, and marking man-made obstacles, ski resorts are reluctant to acknowledge additional responsibility for the safety of their patrons. This is not to say resorts are not concerned about safety; they are very much so, but the point is that as part of their risk management legal strategy, resorts are reluctant to *explicitly* acknowledge additional responsibilities. This strategy extends to terrain park jump designs. Specifically, the NSAA asserts that, due to rider and snow variability, terrain park jump "standards are impossible" [18]. Thus, by this reasoning, engineering design of winter terrain park jumps is likewise impossible, which enables resorts to argue that they are not liable should anything go wrong. In essence, the apparent legal position of the industry is one whereby the resorts provide (possibly unsafe) terrain park jumps for their patrons who, in deciding to use them or not, bear the full responsibility for the consequences.

While the participants must bear primary responsibility for and control over their safety while *using* terrain park jumps, employing engineering design principles to improve the quality and safety of the jumps could prevent or mitigate the potentially tragic consequences of poor patron decisions and otherwise minor accidents. Our central premise is that, although there is significant variability due to snow conditions and rider decisions, these variations are bounded in understandable ways that nevertheless allow engineering designs that accommodate the variability or render it irrelevant. Indeed, based partly on this view, the Committee (F-27) on Snow Skiing of ASTM (previously the American Society for Testing and Materials) is considering bringing recreational winter terrain park jumps within its purview. It appears that engineering design approaches may soon be applied to winter terrain park jumps. Physical modelling of riders using terrain park jumps will then become an important, if not essential, component of this evolution.

Previous work on the modelling and simulation of snow park jumping includes Bohm and Senner [19], Hubbard [20], and McNeil and McNeil [21]. In this paper, the earlier work is reviewed and expanded by treating the terrain park jump as a design problem and exploring the central role that modelling plays in the iterative design process. Several of the most important concepts and design components from a jumper safety point of view are identified and suggestions made that can improve safety and could be easily implemented.

The paper is organized around the iterative design process intended to address the principal hazards of impact and inversion. Section 2 lays out the design problem of the terrain park jump system, identifies its components, and their interaction, and examines the physical constraints and parameters involved. Section 3 addresses the specific hazard associated with impact in landing, introduces the concept of the equivalent fall height (EFH) and uses it to illustrate the potential impact hazards associated with design decisions. This is illustrated using the standard tabletop design revealing fundamental safety issues with this nearly universal form. Section 4 addresses the specific hazard of inversion, and identifies the potential causes of inversion including those that can be induced involuntarily by the design of the approach and takeoff. Example calculations of potential inverting rotations are presented. Section 5 examines how the previously developed material can inform novel terrain park jump designs that limit EFH. Specifically, the concept of the constant EFH landing surface is modelled and example calculations are presented. This section concludes with an illustration of how the calculation of jumper trajectories over each of the terrain park features can be used iteratively to create practical designs with reduced risk of impact and inversion injury. The paper concludes with a summary.

2 Defining the engineering design problem

2.1 General design criteria and constraints

A terrain park jump is a system of interacting components which can generically be labelled as the *start*, the *approach*, the *transition*, the *takeoff*, the *maneuver area*, the *landing*, and the *run-out* (see Fig. 1). Each component has a kinematic input and output that can be modelled using Newton's laws. For example, the input speed for the transition is the output speed of the approach and the output speed of the transition is the input speed for the takeoff and so forth. Terminology is still evolving, however, so the same style jump can be called something different depending on the region where it is built. (For the examples used here, the jump style will be defined graphically.) The most commonly built jump is the standard tabletop jump shown schematically in Fig. 1. For the tabletop jump the maneuver area is intended to be above the deck; however, it is quite common for jumpers to land on the deck; so the deck should be considered part of the landing as well. In the so-called "gap" jump design, there is a deep open gap between the takeoff and the landing. Gap jumps are common in professional competitive events, but are very unusual at recreational resorts serving the general public and so will not be treated here.

Typically the overall performance criterion for the jump is the desired (horizontal) distance of the jump. The length and topographical profile of the terrain park base or parent surface provides a global constraint onto which the jump or jumps must be placed. In general the pitch (the angle of incline) of the terrain park base will not be constant and the analysis of the performance will require numerical solution, but for the sake of illustration, the simple case of a constant pitch for the approach, θ_A, will be treated. The shape of the landing surface will be the subject of a more in-depth analysis. For treating the common tabletop case the pitch of the landing slope will be constant, θ_L. Given a budget constraint of a certain volume of snow, the size of the jump(s) will be constrained. Once the location and size of the jump are determined, one can enumerate the other performance criteria for the various jump components such that the overall performance is met within the global constraints.

Consider the first element of the jump, the start. The start provides a generally flat staging area for the riders to prepare themselves and their equipment and represents the start point for their descent. Design considerations not treated here include having the area be large enough to accommodate the expected traffic flow and having limited access to control the traffic through the jumps as it would be undesirable to have several entry points that could present a collision hazard.

The location of the start point relative to the takeoff provides a limit on the rider's speed that can be attained before takeoff which is an important design parameter. Assuming the rider starts from rest, the maximum speed at takeoff is limited by the difference in elevation between the start and the lip of the takeoff, i.e. $v_{max} \leq \sqrt{2g(y_{start} - y_{lip})}$ where g is the gravitational acceleration constant and y_{start} and y_{lip} are the elevations of the start and lip, respectively. Of course, friction and air drag will lower this value by an amount that depends on the friction coefficient between the snow and ski/snowboard surfaces, the shape of the approach, transition, and takeoff, as well as skier drag coefficient and wind direction and speed. Example calculations for a range of example jumps and kinematic and material parameters will be presented later.

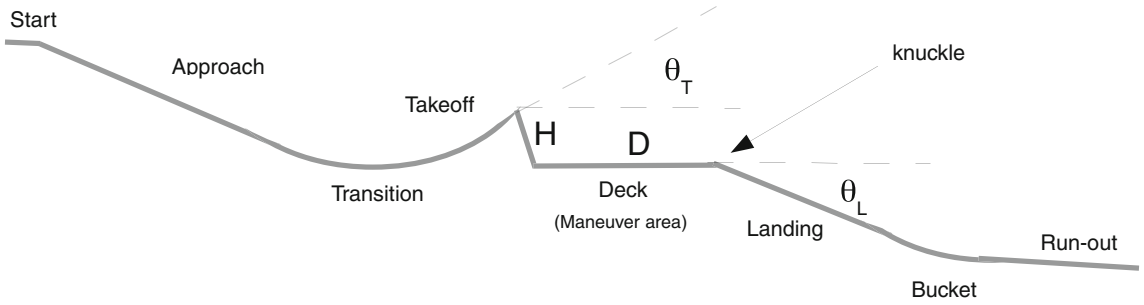

Fig. 1 Geometry of the standard tabletop jump. Although used as an example extensively in this work, the authors do not endorse the tabletop due to its safety problems discussed further in Sect. 3

Once leaving the start, the rider enters the approach or run-in which provides an elevation drop that accelerates the rider to some minimum speed needed for the jump. It is common but not necessary for an approach to have a steep (20–25°) initial "drop-in" region followed by a straight slope of modest pitch ($\sim$10–15°) leading to the transition before takeoff. The purpose of the transition is to provide a smooth region from the downward approach angle to the upward takeoff angle. Therefore, the transition must be curved causing the rider to experience radial acceleration and shifting balance points. Careful consideration must be given to the amount of curvature to avoid excessive radial accelerations, say greater than $2g$, which could throw the rider into an uncontrolled posture [22]. The takeoff provides the last surface of contact for the rider before jumping and therefore the greatest of care must be given to its surface to ensure that it is well groomed and straight. As discussed in detail below, there should be no (concave) curvature in the takeoff which can induce a potentially dangerous inverting rotation. The maneuver area is the region of the jump where the rider is assumed to be in the air; so its properties are often assumed to be less important. This would be true if all jumpers left the takeoff with some minimum speed, but due to the many variables in snow conditions and rider actions, it will often be the case that riders will not maintain sufficient speed into the takeoff to clear the maneuver area; therefore the maneuver area should actually be treated as part of the landing area and its properties examined.

The start of the run-out marks the end of the landing area. The transition between these is called the *bucket*. Through continuous use, the bucket will collect snow that is dislodged from the landing area above by the jumpers. This causes the bucket to creep up the landing area, slowly decreasing the landing area's total length. Designers should accommodate this possibility by increasing the initial design landing length by an amount depending on their local snow conditions and expected use, as well as putting in place monitoring and maintenance procedures for the grooming crews.

2.2 Terminal speed and design considerations for the landing area

The length of the landing area is a critical parameter since overshooting the landing presents a particular impact hazard due to the flatter angle of the run-out. Ideally, the landing area should be designed to accommodate the greatest takeoff speed possible as well as rider "pop" effects which can increase the jump distance. To model the performance of the approach, transition, and takeoff, one requires the dynamic equations describing the center-of-mass motion of the rider while in contact with the snow. Let $y_A(x)$ represent the vertical elevation of the snow surface of the approach, transition, and takeoff where x is the horizontal distance. Assume that the surface is smooth with existing first and second derivatives up to the lip of the takeoff. Assume also that the rider starts from rest and makes no speed-checks, and ignore any motion transverse to the downward direction. This will give a maximum value for the takeoff speed for a given set of physical parameters. The equations of motion for the center-of-mass of the rider while in contact with the surface are given by McNeil and McNeil [21]

$$\frac{\mathrm{d}^2\vec{r}}{\mathrm{d}t^2} = -g\hat{y} + (\hat{n} - \mu\hat{v})N - \eta v^2\hat{v}, \tag{1}$$

where g is the gravitational acceleration constant, $\vec{r} = (x, y)$ is the position vector of the rider suppressing the transverse (z) motion, $\hat{v}$ is the unit velocity vector, $\hat{n}$ is the unit vector normal to the surface, N is the normal force of the surface on the rider, and η is the drag parameter defined below in Eq. 2. The range of physical parameters used in this work are given in Table 1. To treat wind, the velocity vector in the (last) drag term is replaced by the air-rider relative velocity, $\vec{v} - \vec{w}$, where $\vec{w}$ is the wind velocity vector. The drag force is given by Streeter et al. [23],

$$\vec{F}_{\mathrm{drag}} = -\frac{C_{\mathrm{d}}A\rho}{2}v^2\hat{v} = -m\eta v^2\hat{v}, \tag{2}$$

where A is the cross-sectional area of the rider perpendicular to the direction of travel, ρ is the density

Table 1 Physical parameters

Parameter	Symbol	Units	Value range
Acceleration of gravity	g	m/s^2	9.81
Mass of jumper	m	kg	75
Drag coefficient times frontal area of jumper	$C_d A$	m^2	0.279–0.836
Density of air	ρ	kg/m^3	0.85–1.2
Coefficient of kinetic friction	μ	Dimensionless	0.04–0.12
Lift to drag ratio	ρ_{ld}	Dimensionless	0.0–0.1

of air, $\vec{v}$ is the velocity, and C_d is the drag coefficient. Hoerner [24] provides approximate values for the product C_dA for various positions, i.e. for humans standing forward (0.836 m^2), standing sideways (0.557 m^2), and tucked facing forward (0.279 m^2). The density of air, ρ, depends on elevation, Y, and absolute temperature, T, according to the approximate relation [25],

$$\rho(Y,T) = \rho_0 \frac{T_0}{T} e^{-\frac{T_0}{T}\frac{Y}{Y_0}}, \tag{3}$$

where Y is the altitude above sea level in meters, T_0 is the reference temperature (298.15 K), T is the absolute temperature ($T = T_C + 273.15$, where T_C is the temperature in Celsius), $\rho_0 = 1.1839$ kg/m^3, and $Y_0 = 8.772 \times 10^3$ m. For example, this relation gives the air density at an elevation of 3,000 m as $\rho(3{,}000\,\text{m}) = 0.928$ kg/m^3 at $T_C = -10C$.

The normal force is given by McNeil and McNeil [21]

$$N = m(g\cos\theta_A(x) + \kappa(x)v^2), \tag{4}$$

where $\theta_A(x) = -\tan^{-1}(y'_A)$ is the local value of the pitch angle of the hill and $\kappa(x)$ is the local surface curvature,

$$\kappa(x) = \frac{y''_A(x)}{(1+y'_A(x)^2)^{3/2}}. \tag{5}$$

If there were no friction or drag, the maximum speed would be determined simply by the difference in elevation between the start and the lip of the takeoff, i.e. $v_{max} = \sqrt{2g(y_A(0) - y_A(x_{lip}))}$ where x_{lip} is the x-coordinate of the lip of the takeoff. This provides an upper bound to the takeoff speed. Of course, there will always be some friction that reduces the maximum speed by an amount that depends on the shape of the approach and takeoff and the coefficient of kinetic friction which in practice varies between roughly 0.04 and 0.12 [26, 27]. (Note that this is a practical range for the friction coefficient which can be >0.12 for unusually wet circumstances.) For the special case of a straight approach at angle θ_A (constant) with respect to the horizontal, the energy lost per unit length is just the constant frictional force, $\mu mg\cos\theta_A$.

Air drag also reduces the speed at takeoff and provides the velocity dependent force that determines the terminal speed. While the ideal is to have the length of the landing accommodate the maximum takeoff speeds, snow budgets may not allow for very long landings and an engineering trade-off is needed. For the case of a single jump the start point relative to the takeoff can be adjusted to limit the takeoff speed. To calculate the appropriate start point for a given set of conditions, one must solve the equations of motion numerically. One could imagine having two (or more) possible start points and opening the one best suited for the snow conditions. For multiple jumps and for long run-ins, one must consider the possibility of approaching the terminal speed. For such cases the US Terrain Park Council (USTPC) has adopted a landing length design criterion based on a maximal speed of 80% of nominal terminal speed [28]. For the special case of an approach with constant pitch, θ_A fixed, the terminal speed is given by:

$$v_T = \sqrt{\frac{2mg(\sin\theta_A - \mu\cos\theta_A)}{C_dA\rho}}. \tag{6}$$

For example, for a 15° slope using an average rider mass of 75 kg with a low coefficient of friction of $\mu = 0.04$, an air density of 0.928 kg/m^3, and a drag-area of $C_dA = 0.557$ m^2 (appropriate to a rider facing sideways) Eq. 6 gives a terminal speed of $v_T = 24.5$ m/s. Front-facing skiers will have larger drag-area and thus lower terminal speeds.

Note that the terminal speed also provides an upper bound on the size of a jump depending on the shape of the landing surface. Of course, it takes some distance before terminal speed is attained. For the purposes of designing the approach it is necessary to calculate the approach to terminal speed by numerically solving Eq. 1. Figure 2 shows the approach to terminal speed for the range of friction coefficients between $0.04 < \mu < 0.12$. From Fig. 2 for the low friction case, one can see that it takes approximately 150 m for a rider to reach ~20.3 m/s (80% of the terminal speed); so any approaches less than this will meet the USTPC design criterion for the entire range of friction coefficients.

Finally, the width of the landing area must accommodate the possibility that the rider's takeoff is not straight down the jump but includes a component of takeoff velocity transverse to the downhill direction. The approximate transverse distance the rider will land from the downhill center line of the jump will be given by the product of the time-of-flight and this transverse velocity component. Since the time-of-flight is given by the horizontal jump distance divided by the horizontal component of the takeoff velocity (ignoring drag), the transverse deviation will be equal to the horizontal jump distance times the ratio of the transverse to horizontal components

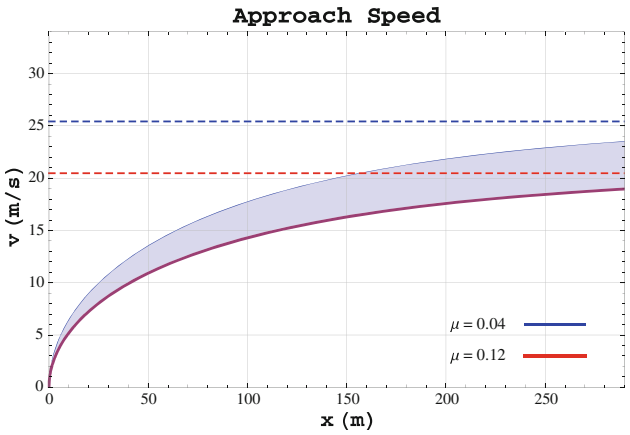

Fig. 2 The approach to terminal velocity as a function of distance down an approach with a constant pitch angle of $\theta_A = 15°$ for the range of kinetic friction coefficients between $0.04 < \mu < 0.12$ obtained by numerically solving Eq. 1. The *dashed lines* represent the terminal speeds for the limiting friction coefficient values

of the takeoff velocity. An approximate limit on this ratio is given by the ratio of the width of the takeoff to the length of the takeoff. In practice, this has not been shown to be a significant safety concern as most riders land with a few meters of the center line, but more on-hill data is needed to better constrain the range of transverse takeoff velocities. A useful guideline is to make the width of the landing area at least three times the width of the takeoff at the design landing point and taper it outward by at least 10° from there to the end of the landing area.

2.3 Jump approach design process

Like many engineering design processes, the jump design process is an iterative one that intimately employs modelling to inform design decisions. A hypothetical design process might take the following steps. First, the performance criteria are established. These may include the target jump distance, minimum radial acceleration in the transition, minimum straight region for the takeoff, and maximum permitted EFH (defined in the next section). Next the constraints are listed, e.g. snow budget and base area on which the jump is to be sited. On a topographical cross sectional profile of the base hill, the snow base and preliminary sketch of the jump with each component is prepared with estimates of all relevant scales such as the snow base depth, start area, length of approach, length and radius of transition, length and width of takeoff, height of lip above start of maneuver area, shape, length and width of the landing area, bucket and run-out. Next, one models the jump design with a mathematical representation of the entire landing surface, defines a range for the physical parameters such as coefficients of friction, drag, and lift, a range for the rider's mass and height, and a range for rider actions such as "pop" speeds (jumping or dropping prior to takeoff) and transverse takeoff angles (relative to straight down the jump). This represents the complete parameter space of interest.

From the mathematical representation of the jump surface, the volume of snow required is calculated and compared with the snow budget. If needed, adjustments to component dimensions can be made, leading, perhaps, to the conclusion that the desired jump size is not compatible with the snow budget. For each set of physical and rider parameters, Newton's laws of motion are solved numerically as described below and the rider's kinematics determined. By repeating the calculation for the various ranges of parameters the entire space of possible rider outcomes is mapped out and the ranges of key performance characteristics calculated such as jump distances, radial accelerations, and EFHs. These may then be compared to the desired performance criteria. From this information design changes can be made and the process repeated until the performance criteria are met within the constraints or a decision is made to revise either the performance criteria (e.g. build a smaller jump), or revise the constraints (e.g. increase the snow budget).

3 Impact hazard

3.1 Equivalent fall height

Clearly, one of the most important factors affecting the relative safety of a jump is the total energy absorbed upon landing. Several authors have used the concept of the *equivalent fall height* (EFH) to characterize this important parameter [20, 29, 30]. Suppose an object falls vertically onto a horizontal surface from a height, h. Ignoring drag, the speed at impact, v, is given by $h = v^2/2g$. On a sloped landing, the impact depends only on the component of the velocity normal to the landing surface, and the relevant energy relation then gives $h = v_\perp^2/2g$. The EFH can be made arbitrarily small by making the angle of the landing surface closely match the angle of the jumper's flight path at landing. The component of the landing velocity normal to the landing surface is given by $v_\perp = v_J \sin(\theta_J - \theta_L)$, where v_J is the jumper's landing speed, θ_J is the jumper's landing angle, and θ_L is the angle of the landing slope. Thus, the EFH is,

$$h = \frac{v_J^2 \sin^2(\theta_J - \theta_L)}{2g}. \quad (7)$$

Due to friction and landing surface distortion, there will be some energy loss associated with the component of landing velocity parallel to the surface. As shown by

McNeil [31], if surface distortion effects are neglected, the maximum energy change, ΔU, including the transverse component is bounded by:

$$\Delta U \leq [2 - (1 - \mu)^2]mgh. \tag{8}$$

This represents the maximum energy absorbed by the jumper, assuming the landing surface absorbs none. Of course, in all realistic cases the surface will experience some distortion which will lower the amount of energy absorbed by the jumper. This effect is carried to the extreme with landing air bags that absorb almost all of the energy. For snow-snowboard/ski surfaces the coefficient of kinetic friction lies in the range $0.04 < \mu < 0.12$ [26]; so the effect of including the tangential component of the change in landing velocity on the absorbed energy is generally small, and the total absorbed energy is well characterized by just the EFH.

To calculate the EFH for an arbitrary jump shape, one must solve the equations of motion for the jumper. The general equations of motion governing the center-of-mass motion including lift and drag are given in Ref. [31]:

$$\frac{\mathrm{d}^2\vec{r}_\mathrm{J}(t)}{\mathrm{d}t^2} = -g\hat{y} - \eta|\vec{v} - \vec{w}|(\vec{v} - \vec{w} - \rho_\mathrm{LD}\,\hat{s} \times (\vec{v} - \vec{w})), \tag{9}$$

where ρ_LD is the lift to drag ratio. Assuming the rider maintains a fixed orientation facing forward, $\hat{s}$ is the unit vector in the "sideways" direction, and the remaining parameters are the same as in Eq. 1. In practice the lift effect is very small ($\sim 1\%$) and depends on the orientation and posture of the jumper in the air; so to simplify matters and get a bound on the lift effect, the lift term in Eq. 9 assumes the jumper maintains his orientation with a constant lift to drag ratio of $\rho_\mathrm{LD} \simeq 0.1$ estimated from the angle of descent of sky-diving snowboarders. Better measurements of this parameter will be necessary for high fidelity modelling. A jumper performing air maneuvers could be modelled using a time-dependent drag/lift ratio, but the net effect should be bounded by the constant ρ_{LD} result. In general, these equations must be solved numerically but, as shown by McNeil [31], for small to medium-sized jumps ($> \sim 12$ m) the drag can be ignored at about the 10% level (and lift effects at the $\sim 1\%$ level) allowing for the closed form analytic solution that is accurate to that level:

$$\vec{v}_\mathrm{J}(t) = (v_{\mathrm{J}x}, v_{\mathrm{J}y}) = v_0 \cos\theta_\mathrm{T}\hat{x} + (v_0 \sin\theta_\mathrm{T} - gt)\hat{y} \tag{10}$$

$$\vec{r}_\mathrm{J}(t) = (x, y) = v_0 \cos\theta_\mathrm{T} t\hat{x} + \left(v_0 \sin\theta_\mathrm{T} t - \frac{1}{2}gt^2\right)\hat{y}, \tag{11}$$

where v_0 is initial speed at takeoff assuming the rider adds no "pop". As shown by Hubbard [20] and McNeil [31], one can treat the jumper's "pop" by adding to the "no-pop" initial velocity, $\vec{v}_0$, an additional velocity component normal to the takeoff surface, $\vec{v}_\mathrm{p} = \{-v_\mathrm{p}\sin\theta_\mathrm{T}, v_\mathrm{p}\cos\theta_\mathrm{T}, 0\}$. This will alter the initial velocity vector (speed and direction) accordingly:

$$\begin{aligned} v_0 &\rightarrow v_{0+\mathrm{p}} = \sqrt{v_0^2 + v_\mathrm{p}^2}, \\ \theta_\mathrm{T} &\rightarrow \theta_{\mathrm{T}+\mathrm{p}} = \theta_\mathrm{T} + \delta\theta_\mathrm{p} \end{aligned} \tag{12}$$

where $\delta\theta_\mathrm{p} = \tan^{-1}(v_\mathrm{p}/v_0)$ and where the $(\cdots + p)$-subscript denotes the initial conditions appropriate to the "pop" case. From field data taken by Shealy et al. [32], "pop" speeds have been shown to vary between $-2.6 < v_\mathrm{p} < +1.2$ m/s [31].

From Eq. 11, one obtains the classic parabolic relation for the jumper's flight path, $y(x)$,

$$y(x) = x\tan\theta_\mathrm{T} - \frac{g}{2v_0^2\cos^2\theta_\mathrm{T}}x^2. \tag{13}$$

As shown in Refs. [20, 22, 30], one can find the jumper's landing angle from the trajectory relation which can be used in the definition of the EFH to derive the following relation for the EFH, $h(x)$, as a function of the landing surface, $y_\mathrm{L}(x)$:

$$\begin{aligned} h(x) = &\left[\frac{x^2}{4\cos^2\theta_\mathrm{T}(x\tan\theta_\mathrm{T} - y_\mathrm{L}(x))} - y_\mathrm{L}(x)\right] \\ &\times \sin^2\left[\tan^{-1}\left(\frac{2y_\mathrm{L}(x)}{x} - \tan\theta_\mathrm{T}\right) - \tan^{-1}y'_\mathrm{L}(x)\right]. \end{aligned} \tag{14}$$

where $\theta_\mathrm{L}(x) = \tan^{-1}y'_\mathrm{L}(x)$ has been used.

This expression for EFH characterizes the severity of impact upon landing as a function of the horizontal distance of every jump. In fact, once a rider leaves the takeoff with a given initial velocity, his flight path, landing point and EFH are determined. When drag and lift are neglected, simple analytic expressions such as Eq. 14 for the EFH can be obtained; however, it is straightforward to solve the Eq. 9 numerically to determine $h(x)$ including drag and lift effects.

The most common recreational jump built is the standard tabletop, shown schematically in Fig. 1. Most experienced tabletop jumpers quickly learn that there is 'sweet spot' just past the knuckle that is the ideal landing area resulting in a light landing impact. Using Eq. 14, one can explore the EFH for a variety of hypothetical tabletop jumps. The tabletop jump is parametrized by the takeoff angle, θ_T, deck length, D, takeoff lip height, H, and landing surface angle, θ_L. The tabletop design is evaluated because of its current widespread use and analytic simplicity; however, as shall be shown below, this design is not optimal for limiting EFH. For the special case of the tabletop jump the landing surface is described by the function,

$$y_L(x) = \begin{cases} -\tan\theta_L(x-D) - H, & x \geq D \\ -H, & x < D. \end{cases} \quad (15)$$

where H is the height of the takeoff above the deck, D is the deck length and θ_L is the landing angle as shown in Fig. 1. As shown by Swedberg and Hubbard [29], using this form, one can obtain the EFH function specifically for the tabletop jump:

$$h_{tt}(x) = \begin{cases} \cos^2\theta_L(H - D\tan\theta_L) + \frac{x^2\sin^2(\theta_L+\theta_T)}{4\cos^2\theta_T[x(\tan\theta_T+\tan\theta_L)+H-D\tan\theta_L]}, & x \geq D \\ H + \frac{x^2\tan^2\theta_T}{4(x\tan\theta_T+H)} & x < D. \end{cases} \quad (16)$$

One can examine the sensitivity of the EFH of the tabletop jump by varying each of the relevant parameters, $\{\theta_T, H, D, \theta_L\}$, keeping the remaining parameters fixed. The resulting EFH function can also be compared to some design criterion.

A natural question that arises is: how small a value for h is small enough? To answer this question it is important to realize that good designs do not limit themselves to best case scenarios. As the EFH rises the probability of serious injury rises with it. Clearly, subjecting a person to an EFH of 10 m would be considered dangerous. Even if the jumper is in complete control and lands in the best possible body configuration, serious injury is likely to occur when the EFH is this large. Similarly, an EFH of 3 m is probably still too large, not because an athletic ski jumper under ideal conditions could not possibly survive an impact with this EFH, but rather because if anything deviated from the best case scenario (slipping on takeoff, getting one's skis or board crossed in flight, etc.) then serious injury could still occur. Another basis to inform an EFH criterion is the ability of the jumper to control his descent after landing. Recent experiments on jumpers have shown that above about $h = 1.5$ m, the ability of a young athletic human to absorb the vertical impulse and maintain control without the knees buckling is compromised. This is the basis for the USTPC criterion of a maximum acceptable EFH of 1.5 m [28]. Landing areas meeting this criterion shall be referred to as the "soft-landing" region of the jump.

Figure 3a shows the sensitivity of the EFH to H, the height of the lip of the takeoff, while fixing the remaining parameters at: $\{\theta_T = 20°, D = 6.1\text{ m } (20\text{ ft}), \theta_L = 30°\}$. For the case of $H = 1.0$ m the EFH for landing on the deck is below 1.5 m for the entire deck length. Beyond the deck the EFH drops rapidly for landing on the sloped landing area before increasing to 1.5 m at a distance of about 16 m. Thus, for the low deck height of $H = 1.0$ m, the EFH exceeds the USTPC criterion value only beyond 16 m. This constitutes a landing zone with a 10 m long soft-landing region. For the larger deck height of $H = 2.0$ m, the EFH exceeds 1.5 m for the entire length of the deck before dropping to acceptable levels after the knuckle but increasing quickly again to 1.5 m at about 13 m. Thus the soft-landing region for the large deck height case is more narrow, about 7 m long, and in addition to the hazard of landing short of the knuckle one would expect some jumpers to land outside this soft-landing zone.

Figure 3b shows the sensitivity of the EFH to θ_T, the takeoff angle, while fixing the remaining parameters at: $\{H = 1.5\text{ m}, D = 6.1\text{ m}, \theta_L = 30°\}$. Since the lip height in this case is 1.5 m already, in both takeoff angle cases the EFH for landing on the deck exceeds 1.5 m the entire length of the deck. For the $\theta_T = 10°$ case, the EFH for landing on the sloped landing area drops to a very small value before increasing to 1.5 m again at a distance of about 18 m. Thus, the soft-landing region for this case is fairly long, $\sim$12 m. For the steeper takeoff angle of $\theta_T = 30°$, the EFH rises quickly along the deck before dramatically dropping to acceptable levels after the knuckle but increasing to 1.5 m again at about 12 m. Thus the soft landing region for this jump is about 6 m long and one would expect some jumpers to land outside this zone.

Figure 4a shows the sensitivity of the EFH to θ_L, the angle of the landing surface (here assumed constant), while fixing the remaining parameters at: $\{H = 1.5\text{ m}, D = 6.1\text{ m}, \theta_T = 20°\}$. The landing angle does not affect the EFH for landing on the deck so for both cases the EFH for landing on the deck rises with distance to about 1.8 m at the knuckle. For the case of $\theta_L = 10°$ the EFH for landing on the sloped landing area starts at about 1.1 m just after the knuckle and increases quickly to 1.5 m at a distance of about 9 m. Thus, the soft-landing region for this case is relatively short, only $\sim$3 m. For the steeper landing angle of $\theta_L = 30°$, the EFH starts considerably lower and rises to 1.5 m at about 14 m. Thus, the soft-landing region for this case is fairly long, $\sim$8 m; so it would appear that the greater risk of having an EFH >1.5 m would arise from landing before the knuckle.

Figure 4b shows the sensitivity of the EFH to D, the deck length, while fixing the remaining parameters at: $\{h = 1.5\text{ m}, \theta_T = 20°, \theta_L = 30°\}$. The first case is for $D = 3$ m (10 ft). The EFH rises from 1.5 to 1.6 m along the deck

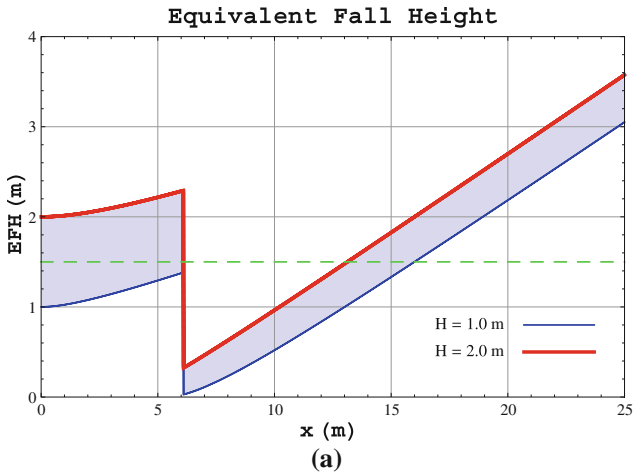

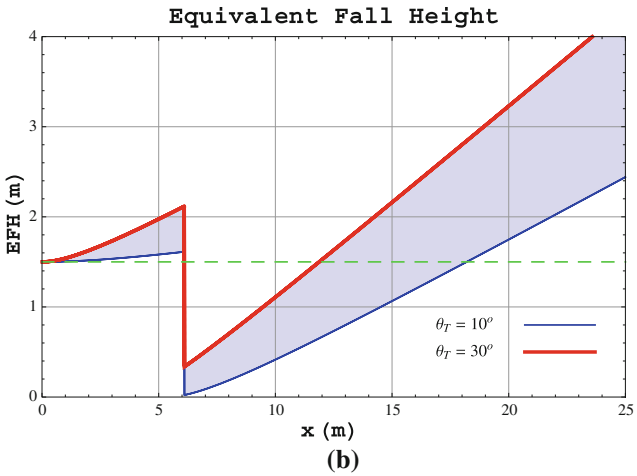

Fig. 3 Tabletop EFH versus jump distance x for **a** varying the takeoff lip height, $1 \leq H \leq 2$ m, with $\theta_T = 20°$, $D = 6.1$ m, and $\theta_L = 30°$ fixed, and **b** varying the takeoff angle, $10° \leq \theta_T \leq 30°$, with $D = 6.1$ m, $H = 1.5$ m, and $\theta_L = 30°$ fixed. The *dashed* (*green*) *line* marks the USTPC criterion value for the maximum allowable EFH (1.5 m) (colour figure online)

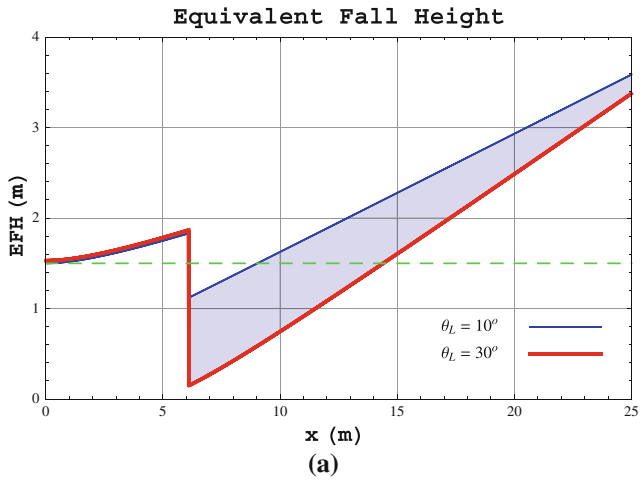

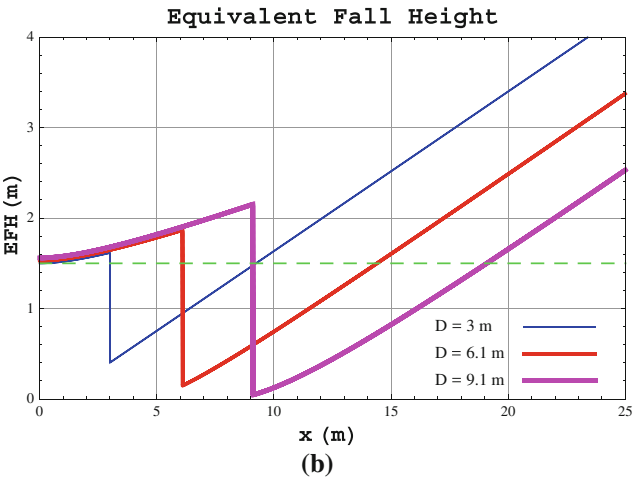

Fig. 4 EFH versus jump distance x for landing on a constant downward slope landing for **a** varying the landing angle, $10° \leq \theta_L \leq 30°$, with $D = 6.1$ m $H = 1.5$ m, and $\theta_T = 20°$ fixed, and **b** varying the deck length, $D = 3.0$ m, $D = 6.1$ m, and $D = 9.1$ m with $\theta_T = 20°$, $H = 1.5$ m, and $\theta_L = 30°$ fixed. The *dashed* (*green*) *line* marks the USTPC criterion value for the maximum allowable EFH (1.5 m) (colour figure online)

before dropping to about 0.4 m after the deck and then rising to 1.5 m at a distance of 9 m. Thus, the soft landing region for this case is about 6 m long. For the deck length of $D = 6.1$ m (20 ft), the EFH rises to about 1.8 m at the knuckle before dropping to 0.2 m just after the knuckle and then rising to 1.5 m at a distance of 14 m. Thus, the soft landing region for this case is about 8 m long. For the deck length of $D = 9.1$ m (30 ft), the EFH rises to about 2.2 m at the knuckle before dropping to $\sim$0.1 m just after the knuckle and then rising to 1.5 m at a distance of $\sim$19 m. Thus the soft-landing region for this case is quite long, $\sim$10 m, but the EFH for landing before the knuckle significantly exceeds the USTPC criterion value.

In most resorts the jumps are not engineered and new jumps are empirically tested by professional staff riders. Due to their considerable experience test jumpers are seldom injured, yet such blind tests present a hazard to staff that could be avoided with a relatively simple engineering analysis such as presented here.

If a snow park jump can be designed with inherently small values of EFH and large soft landing regions, then many jump injuries can be avoided or their severity reduced since energy absorbed upon landing is reduced. An examination of the EFH for the tabletop jump shown in Fig. 3 and studied in detail by Swedberg and Hubbard [29] shows a disturbing trend in that the EFH increases roughly linearly as jump length increases despite adjustments to lip height, H, deck length, D, and landing slope angle θ_L. As these results show, landing just before the knuckle or well after the soft landing region can result in large EFHs and

thus present a greater risk for an impact-related injury. The straight landing used in tabletop designs will always have an increasing EFH with jump distance suggesting that alternative landing shapes should be seriously considered.

3.2 Interacting parameters: approach length, takeoff speed and landing length

As discussed above, the primary impact hazards presented by the standard tabletop jump are either landing too short (before the knuckle) or too long, especially beyond the landing area. Indeed, overshooting the landing area is one of the least desirable outcomes of a jump. Of course, the distance of a jump depends on the takeoff velocity (both direction and magnitude). (As discussed above and in Refs. [20, 31], the effect of the rider adding "pop" merely modifies the initial velocity according to Eq. 12.) As seen from Eq. 1, the (no-pop) takeoff speed depends on the shape of the surface up to the end of the takeoff ramp and the physical parameters determining friction and drag. This implies that there will be a coupling of the performance characteristics of the components.

For example, the length of the approach will determine the range of takeoff speeds which, in turn, will determine the range of landing distances. In the examples below the tabletop jump parameters were fixed as follows: $\{\theta_A = 15^\circ, L_{TO} = 4.0\,\text{m}, \theta_T = 20^\circ, H = 1.5\,\text{m}, D = 9.1\,\text{m}, \theta_L = 30^\circ\}$, where L_{TO} is the length of the takeoff ramp. The physical parameters are listed in Table 1 with the following specific values: $\{C_dA = 0.557\,\text{m}^2, \rho = 0.90\,\text{kg/m}^3, m = 75\,\text{kg}\}$. Figure 5a shows the takeoff speed versus the length of the approach obtained by numerically solving Eq. 1 for this hypothetical tabletop jump. Figure 5b shows the resulting total horizontal jump distance, x_J, for the full range of friction coefficients. These figures can be used to inform the jump designer's decision regarding the length of the approach and length of the landing. For the low friction case a modest approach length of $\sim$40 m will provide enough takeoff speed to reach the start of the landing; however, if the snow conditions change such as to increase the friction coefficient, then there is a strong likelihood that riders will land on the deck and be subjected to a large EFH as discussed previously. To avoid this outcome for this set of example parameters allowing an approach length of at least $\sim$75 m will provide sufficient takeoff speed to reach the landing area under the large friction conditions (without having to add 'pop').

Consider next the length of the landing area. As an example suppose an approach length of 100 m. Under large friction conditions the landing distance is about 18 m, or 9 m (horizontal) beyond the knuckle. Thus, having a landing length (measured along the hill) of $(9.0/\cos\theta_L)\,\text{m} = 10.4$ m will accommodate all jumpers under the high friction condition. However, if the snow conditions change and the coefficient of friction drops, there is a strong likelihood that jumpers who fail to check their speed will land beyond the landing area. Since the maximum jump distance for a 100 m approach length for this takeoff angle under low friction conditions is about 32 m, the landing length should be a least $(32.0/\cos\theta_L)\,\text{m} \simeq 37$ m. If the snow budget is insufficient for that length for the landing area, the designer can try a different takeoff angle or deck length or other parameter thereby continuing the iterative engineering design process.

Next, the dependence of the peak radial acceleration in the transition on the length of the approach, L_A, is

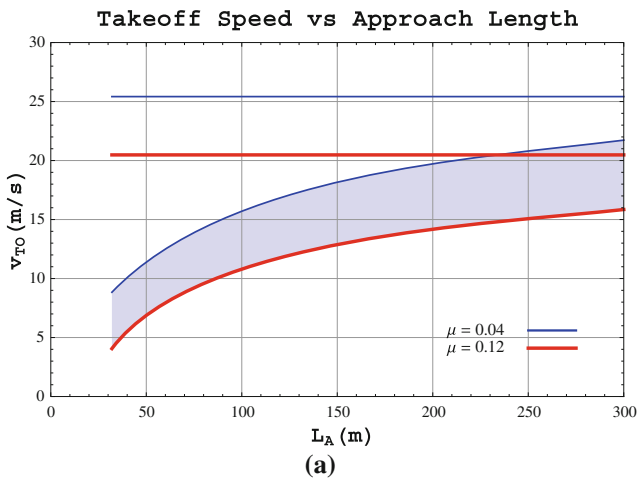

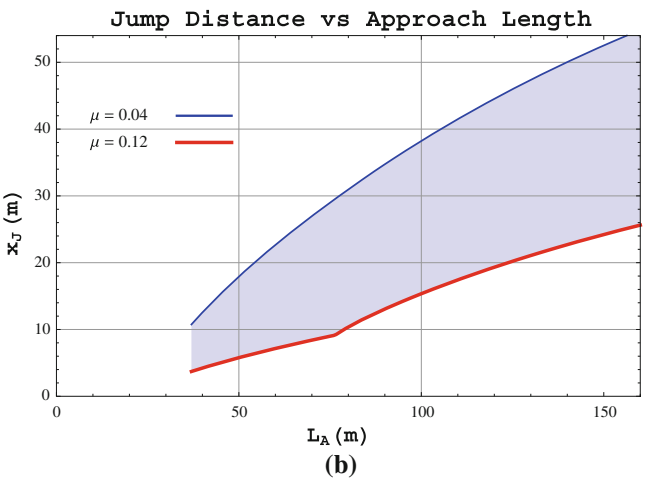

Fig. 5 **a** Takeoff speed and **b** the landing distance as a function of the length of the approach, L_A, for a standard tabletop jump for the full range of friction coefficient, $0.04 \le \mu \le 0.12$. For both curves, the tabletop jump parameters were fixed as follows: $\{\theta_A = 15^\circ, L_{TO} = 4.0\,\text{m}, \theta_T = 20^\circ, H = 1.5\,\text{m}, D = 9.1\,\text{m}, \theta_L = 30^\circ\}$, and the remaining physical parameters were: $\{C_dA = 0.557\,\text{m}^2, \rho = 0.90\,\text{kg/m}^3, m = 75\,\text{kg}\}$

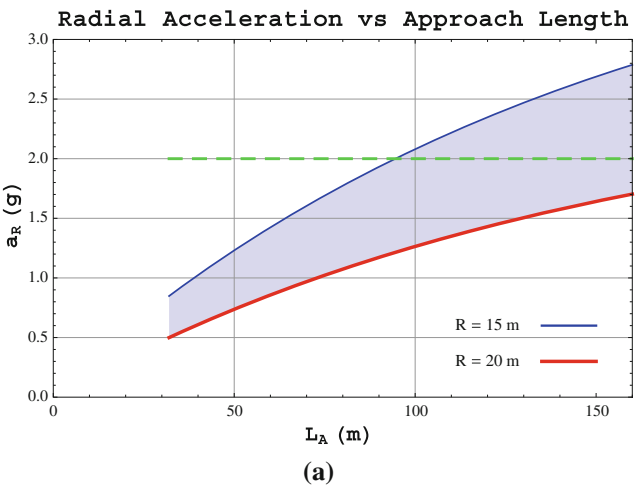

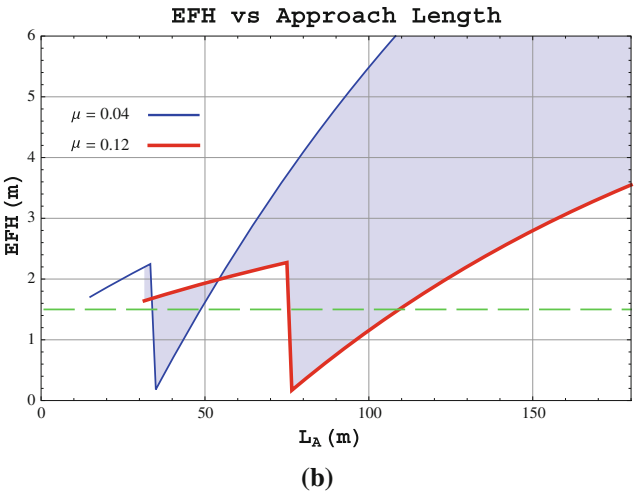

Fig. 6 **a** Peak radial acceleration in the transition for $R = 15$ m and $R = 20$ m as a function of the length of the approach, L_A, for a standard tabletop jump with the friction coefficient fixed at its lower limit, $\mu = 0.04$, and **b** equivalent fall height, h, as a function of the length of the approach, L_A with the friction coefficient varied between $0.04 \leq \mu \leq 0.12$. For both figures, the remaining tabletop jump parameters were fixed as follows: $\{\theta_A = 15^\circ, L_{TO} = 4.0\,\text{m}, \theta_T = 20^\circ, H = 1.5\,\text{m}, D = 9.1\,\text{m}, \theta_L = 30^\circ\}$, and the remaining physical parameters were: $\{C_dA = 0.557\,\text{m}^2, \rho = 0.90\,\text{kg/m}^3, m = 75\,\text{kg}\}$

examined. Figure 6a shows the peak radial acceleration in the transition measured in units of the acceleration constant, g, versus the length of the approach for the full range of friction coefficients, $0.04 \leq \mu \leq 0.12$ with the remaining parameters fixed as described previously. For the transition radius of 15 m the radial acceleration exceeds the USTPC recommended maximum of 2 g's at an approach length of about 90 m while the 20 m transition radius will allow approach lengths greater than about 150 m.

Finally, the dependence of the EFH on the length of the approach, L_A, is examined. Figure 6b shows the EFH versus the length of the approach for the full range of friction coefficients, $0.04 \leq \mu \leq 0.12$ with the remaining parameters (given in the figure caption) fixed. One can clearly identify the approach length that provides sufficient takeoff speed to clear the knuckle. For the low friction case this occurs at an approach distance of only 45 m while for the high friction case an approach length of about 95 m is required. This figure clearly emphasizes the dilemma that the jump designer faces when constrained to the simple tabletop form. For both low and high friction cases there exist regions where the EFH is below 1.5 m; however, there is no single value of the approach length for which the EFH is below 1.5 m for *both* friction extremes. One can manage this situation by having multiple start points depending on the snow conditions, but this requires that resorts building such jumps be able to measure the friction coefficient and devise plans to monitor it continuously. These considerations strongly suggest that the jump designer explore other options for landing shapes for jumps of this size (9.1 m) or larger.

There is an insidious psychological effect that infects the tabletop design as well. The large EFH arising from landing short of knuckle on a tabletop creates a psychological avoidance response in jumpers. To avoid hard knuckle landings jumpers tend to take the jump faster than they might otherwise do which in turn increases the risk of overshooting the landing with potentially even worse outcomes than landing on the knuckle. The narrower the region of "soft" landing, the greater the risk.

While the preceding analysis was performed for the standard tabletop design, it should be emphasized that any design shape can be similarly analysed.

4 Inversion hazard

One especially hazardous situation occurs when the jumper lands in an inverted position which can lead to catastrophic injury or death from spinal cord trauma. While jumpers can execute inverted maneuvers intentionally, concave curvature in the takeoff can lead to involuntary inversion. Curvature in the takeoff can be intentionally built or can be arise through heavy use. Understanding the dynamics of a jumper riding over a takeoff with concave curvature is necessary to developing designs and maintenance procedures which mitigate, if not eliminate, this hazard.

McNeil [33] modelled the inverting effect of a curved takeoff by treating the jumper as a rigid body which approximates a stiff-legged jumper. This work is briefly reviewed here. For a simple illustrative example, consider the inverting rotation for trajectories calculated from the

standard tabletop jump which is the most widely used design, although not built to any standard. The mathematical simplicity of this jump shape allows for similarly simple expressions for the quantities of interest. Results for more general shapes are straightforward but may require numerical solution. In the previous section it was shown that the tabletop design is not optimal from the point of view of its potential impact hazard as characterized by a large EFH as discussed above (see also Refs. [20–22, 29]). However, the focus here is exclusively on the interaction of the jumper with the takeoff. The other components of the jump only affect the time of flight and impact as discussed above. Ignoring drag, for a jump of horizontal distance of x_L the time of flight is given by:

$$t_F = \frac{x_L}{v_0 \cos\theta_T}. \tag{17}$$

The concavity of the takeoff is characterized by the radius of curvature, R_{TO}. Assuming the rider is a rigid body during takeoff implies that the takeoff velocity is parallel to the takeoff ramp surface at its end (the lip). The angular speed for inversion induced by the curved takeoff is given by the takeoff speed, v_0, divided by the radius of curvature $\omega = v_0/R_{TO}$ where the inverting rotation is about an axis normal to the plane of the jumper's trajectory. This can be understood by imagining a rider executing a full vertical circle at constant speed who must rotate by 2π in each revolution. Once the jumper leaves the surface, neglecting drag and lift, no further torques can be exerted on the jumper so his/her angular momentum is conserved. Under the rigid body assumption, the moment of inertia is fixed so the angular velocity is also fixed. Under these conditions, the total inverting rotation is given by the angular velocity times the time of flight,

$$\phi = \frac{x_L}{R_{TO} \cos\theta_T}. \tag{18}$$

One notes that the inverting rotation is proportional to the horizontal jump distance and inversely proportional to the radius of curvature; so smaller jumps can tolerate a smaller radius of curvature. The magnitude of the total backward inverting angle relative to the landing surface under the rigid body assumption is thus,

$$\Phi = \phi + \theta_T + \theta_L. \tag{19}$$

Non-rigid body motion, arising for example by the rider executing a maneuver in the air, will change the rider's moment of inertia and the rotational speed will not be constant. Modelling such cases requires a detailed analysis of the maneuver's affect on the moment of inertia during the jump. It should be noted that the most common maneuver is the "grab" which will tend to reduce the moment of inertia thereby increasing the inverting angle.

For jumps with relatively large takeoff and landing angles $\theta_T = \theta_L \sim 30°$, very little additional inverting rotation can result in a potentially disastrous landing on the head or neck. In the example medium-sized tabletop ($\sim$6 m) jump treated in Ref. [33] the takeoff was found to have a radius of curvature of about 8.1 m. For an approximate takeoff speed of 7.2 m/s, the inverting angle was estimated to be about 63° which resulted in the (rigid-body) rider landing in an inverted position at the potentially dangerous angle of 126° with respect to the landing surface normal.

What are the design implications? Clearly, curvature should be avoided in the last few meters of the takeoff, but how long should the straight section of the takeoff be? As can be seen from Fig. 1 the takeoff immediately follows the transition which takes the rider from a predominantly downhill direction to the upward direction of the takeoff. The straight section of the takeoff ramp should be long enough to allow the rider to recover from the transition. The USTPC has proposed that the straight section of the takeoff be at least the nominal design takeoff speed times 1.5 human reaction times, or about 0.3 s. This is close to the standard used for nordic jumps which is 0.25 s times the nominal takeoff speed. For the medium jump treated in Ref. [33] the nominal takeoff speed was about 7.2 m/s which implies a recommended minimum straight section of takeoff of about 2.2 m.

5 Designing tomorrow's terrain park jump

Previously it was shown that the impact risk associated with landing is naturally quantified by the EFH, and that a "soft" landing arising from a correspondingly small EFH is possible if the jumper path and landing surface have nearly the same angle at the point of impact.

Although the most commonly used jump, the tabletop, was used in the previous example calculations of impact and inversion hazards, it was emphasized that this was not intended to be an endorsement of this kind of jump. As shown above, tabletop jumps have narrow "soft landing" regions and, even if built for such landings under one set of snow conditions, these can change to a "hard landing" when the snow conditions change. Nevertheless, tabletops continue to be built. This may be due their ease of construction, the vast experience builders now have with that form, and the fact that this is what everyone else is doing, a form of safety in numbers. Tabletops are indeed relatively simple to design and fabricate with the only design decisions being the quantities: L_A, the length of the approach with some arbitrary curved transition; L_T, the length of the takeoff; θ_T, the angle of the takeoff; H, the height from the lip of the takeoff to the (generally horizontal) deck surface; D, the length of the deck surface; θ_L, the angle of the

intended landing surface; and L_L, the length of the intended landing region. Typically, the base or parent slope upon which the jump is sited is fairly straight and inclined at some average angle θ_A which is used for the approach angle to conserve snow. The tabletop is relatively easy to fabricate due to the many straight lines which can be constructed readily with modern grooming equipment.

But, while it may be easy to build a landing region consisting only of two straight line segments, as shown above the resulting jump is not necessarily ideal from the perspective of impact hazards. Simplicity of design (in the sense of few choices to be made) thus carries an associated penalty: it can subject the jumper to large impacts on landing. In Sect. 3 above, it was shown that the EFH function associated with such a generic tabletop jump has undesirable characteristics. Specifically, on medium to large-sized jumps, the EFH is small only in a relatively narrow range of takeoff speeds (and even this requires the correct choice of the intended landing region surface angle). Furthermore, the EFH can be dangerously large when landing occurs at the end of the deck or beyond the intended landing region. Thus tabletop jumps will have acceptable EFH's only in too narrow a region that can change dramatically with the snow conditions. This places large demands on the jumper to manage the takeoff velocity precisely within a narrow range and too large a penalty (severe and possibly dangerous impacts) if the velocity is outside this range for whatever reason. Indeed, as shown in Sect. 3 there may be conditions where the approach length provides an acceptable takeoff speed under one set of snow conditions, only to be unacceptable when the snow conditions change. As shown previously, this sensitivity arises from the constraint that the deck and landing surface be straight. The possibility of relaxing this constraint is now addressed by considering curved landing surfaces that, by design, provide acceptable EFH independent of the takeoff speed up to the limits of space and fabrication capabilities.

The benefits of such a surface are clear, but how might this be done? The mathematical condition for a landing surface shape that produces an acceptable EFH begins with Eq. 7 in which EFH vanishes when the jumper path and landing surface have the same angle at the point of impact. A more complete discussion of the theory behind calculation of safer jump landing surface shapes is provided by Hubbard [20]. In summarizing, a condition on the surface shape, $y_L(x)$, is sought such that the EFH is limited to a specific value h at all values of x. Indeed, Eq. 14 is such a condition, although in that form it was used to calculate the EFH.

Solving for $y'_L(x)$ from Eq. 14, one can obtain an expression for the derivative of the landing surface which is now interpreted as a differential equation constraining the landing surface,

$$y'_L(x) = \tan\left[\tan^{-1}\left(\frac{2y_L(x)}{x} - \tan\theta_T\right) + \sin^{-1}\sqrt{\frac{h}{\frac{x^2}{4(x\tan\theta_T - y_L(x))\cos^2\theta_T} - y_L(x)}}\right]. \quad (20)$$

In Eq. 20, which has been called the "safe slope differential equation" [20], the first derivative of the landing surface function is a function of two variables (x and $y_L(x)$) and three constant parameters (g, θ_T and h). Since no jump can ever be definitively called "safe", in this work such surfaces will be referred to as "constant EFH" surfaces. Any surface $y_L(x)$ that satisfies this differential equation imparts to an impacting jumper a value of EFH equal to h no matter what the takeoff speed v_0 and consequent landing position. This surface has had its impact safety designed into it through the specification of a particular value h of EFH that parametrizes the surface. The fact that the surface shape is insensitive to takeoff velocity v_0 is made manifest by the absence of v_0 in Eq. 20. Also note that Eq. 20 is general in that the EFH value, h, could in fact be a (smooth) function of x thereby giving the jump designer freedom to tune the EFH everywhere.

Shealy and others [18, 32, 34, 35] have questioned the practicality of building such a jump due to "uncontrollable factors" such as jumper discretion (e.g. "pop") leading to variations in takeoff angle and drag variations in flight, snow variability (snowfall and melt), temperature variations, etc. However, recent studies by McNeil [31] and Hubbard and Swedberg [30] of these so-called "uncontrollable factors" have shown, to the contrary, that these factors are bounded in understandable ways that can be addressed in the design. Thus the idea that such variability precludes the use of engineering design is not supported. Indeed, much of the present paper continues to illustrate this fact: design of jumps limiting EFH can proceed while explicitly accounting for such factors or rendering the impact of such variability largely irrelevant.

To find specific instances of constant EFH surface shapes one must solve Eq. 20 by numerical integration. First, one must specify the values of the parameters θ_0 and h, and, since it is a *first order* differential equation, one must also choose a specific boundary condition $y_L(x_F)$ at some value of x_F. For technical reasons [22] related to the behaviour of the equation at small values of x, it is necessary to integrate Eq. 20 backward, rather than forward, in x; so x_F is taken to be the terminal point for the constant EFH surface. The arbitrariness of the boundary condition means that there is an infinite number of such solutions for fixed h parametrized by $y_L(x_F)$.

The choice of the implemented value of h is up to the designer, but the designer needs to make an informed and scientifically supportable choice. This decision can be

defended and communicated to the users of the jump so that they are better informed as to the risks they undertake in using the jump. The USTPC has adopted a 1.5 m maximum EFH based on the degree of knee flex in snowboarders landing on flat surfaces. Regardless of the choice, however, it is important to be clear; constant EFH landing surfaces will not eliminate serious injuries from jumping, but they can reduce the likelihood of such injuries and decrease the severity of injury should something go wrong. This can be especially important in the event the jumper becomes inverted.

One of the consistent lessons learned from the epidemiological studies is that beginners are at significantly greater risk than the more skilled riders [13]. In part to address this problem, resorts have developed ski and snowboarding schools including "progressive parks" with varying levels of difficulty and risk. Constant EFH landing surfaces would be especially well-suited to progressive terrain parks which are intended to develop riders from beginner to more advanced skill levels. Currently, such progressive parks start with simple rollers over which a rider can "catch some air", and then progress to a series of tabletop jumps with increasing deck lengths. The novice rider is then confronted with the requirement of a quantum leap in skill level in progressing from one tabletop to the next larger size with considerably greater risk for injury. The constant EFH surface, on the other hand, provides the opportunity for continuous development of skill level from the smallest to the largest jump length attainable on a slope of fixed pitch while mitigating impact risks through the properties of the constant EFH surface.

Figure 7 shows two samplings (as leaves from a book) of the infinite family of constant EFH landing surfaces for the two values of $h = 1.0$ and 1.5 m with $\theta_T = 10°$ fixed. Similarly, Fig. 8 show two samplings of constant EFH landing surfaces for the combinations of $h = 1.0$ and 1.5 m with $\theta_T = 25°$ fixed. Each set of landing surfaces extends over the range $0 < x < 30$ m, with the boundary conditions for each constant EFH surface given by values of y_L at $x_F = 30$ m evenly distributed from -6 m $> y_L > -12$ m. For each pair of design values of h and θ_T, the family of surfaces asymptotically emanates from the same point, called the "singular point" [22] where the argument of the tangent function in Eq. 20 goes through $\pi/2$. Every one of the landing surfaces in each of Figs. 7 and 8 produces the same EFH (either $h = 1.0$ m or $h = 1.5$ m) independent of jumper takeoff speed.

Note that the constant EFH landing landing surfaces in Figs. 7 and 8 do not look like tabletops with cusps. Every smooth constant EFH landing surface has a monotonically decreasing slope (becoming more and more negative and eventually steeper and steeper). All surfaces become steeper at larger values of x. Of course, there is a practical limit to the steepness of the landing surface determined by the capabilities of the grooming and fabricating equipment. As discussed more completely below, most commonly used grooming machines today can function only up to an incline angle of about 30°.

Figures 7 and 8 display the sensitivity of the families of constant EFH landing landing surfaces to the two design parameters h and θ_T. Generally speaking, as the value of h increases (e.g. Fig. 7a, b), the family of constant EFH curves shifts downward on the left, near $x = 0$, and become slightly "flatter". As the takeoff angle θ_T increases (e.g. Figs. 7a to 8a), the family becomes significantly "rounder", without shifting downward near the singular point.

The constant EFH landing surfaces in the figures were calculated by integrating Eq. 20 which assumes no drag. It is important to emphasize that similar safe surfaces incorporating air drag can be calculated and that these differ

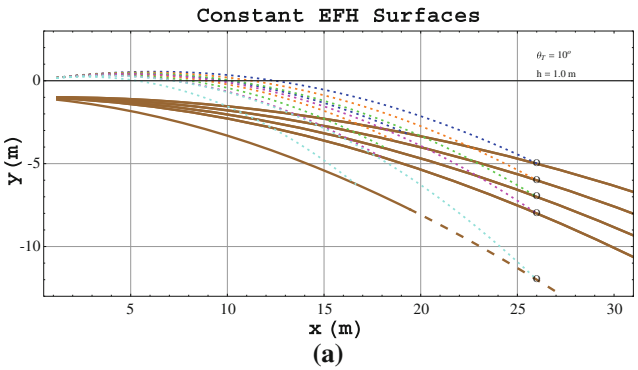

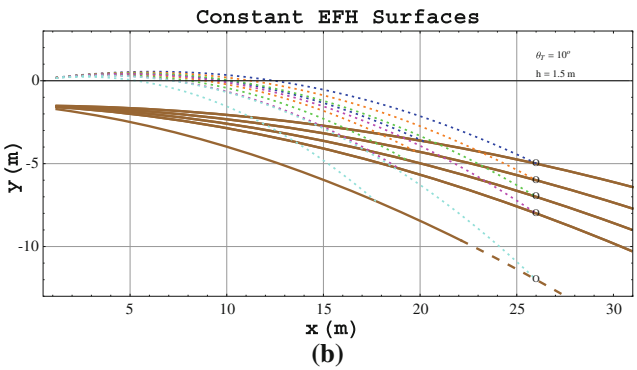

Fig. 7 Constant EFH landing surfaces for **a** $h = 1.0$ m and **b** $h = 1.5$ m with $\theta_T = 10°$ fixed. Also shown are sets of possible jumper paths, the uppermost of which corresponds to a 26 m horizontal jump distance requiring a takeoff speed of 18.9 m/s. The *circles* mark the location of the boundary conditions used to integrate Eq. 20 to obtain the constant EFH surface. The $\theta_L = 30°$ point on the constant EFH surfaces is identified by a *dashed line* beyond which fabrication is impractical with present snow grooming equipment without use of a winch

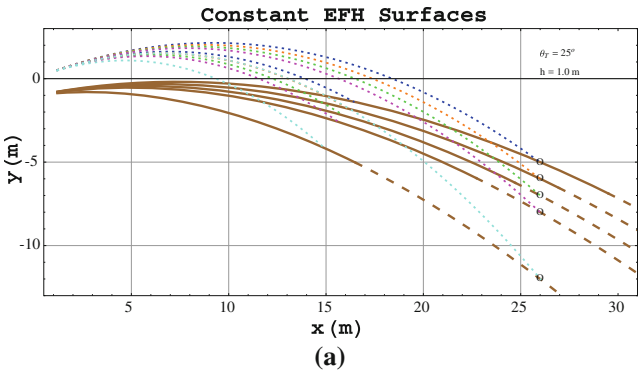

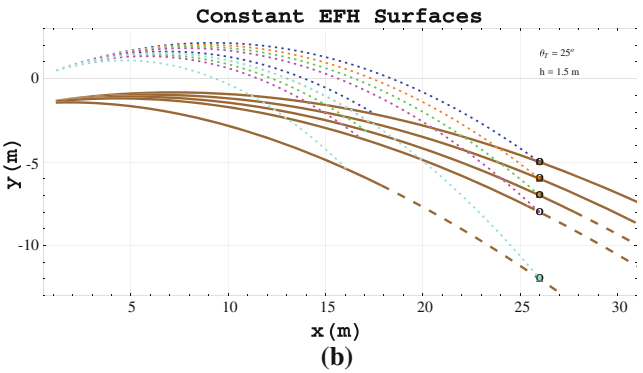

Fig. 8 Constant EFH landing surfaces for **a** $h = 1.0$ m and **b** $h = 1.5$ m with $\theta_T = 25°$ fixed. Also shown are sets of possible jumper paths (*dotted*), the uppermost of which corresponds to a 26 m horizontal jump distance at a takeoff speed of 15.35 m/s. The *circles* mark the location of the boundary conditions used to integrate Eq. 20 to obtain the constant EFH surface. The $\theta_L = 30°$ point on the constant EFH surfaces is identified by a *dashed line* beyond which fabrication is impractical with present snow grooming equipment without use of a winch

only marginally from the surfaces, shown in Figs. 7 and 8, that satisfy Eq. 20. However, it is not possible to show the analytic differential equation for the surface analogous to Eq. 20 in the presence of drag. The essential modification is the following: during the integration of the constant EFH surface backward, because of drag there is no analytic expression for the takeoff velocity required to pass through the present point on the surface, nor for the impact velocity at that point. Instead, these velocities must be calculated numerically with a shooting technique, making the calculations more laborious but no less accurate. Later the effect of including drag on the EFH is shown to be very small for surfaces calculated using Eq. 20.

Several practical design considerations must be kept in mind. First, the present generation of snowcats without use of a winch are not able to fabricate and easily maintain snow surfaces steeper than roughly 30°. Thus only those portions of the constant EFH landing surfaces satisfying $\theta_L \leq 30°$, can be created and maintained in practice. It is impractical to view the segments of the surfaces shown in Fig. 8 as desirable solutions in ranges where their angles exceed 30°. In each surface shown in Figs. 7 and 8, the segments where the slope of the surface exceeds 30° are indicated by dashed lines.

Secondly, although all the surfaces shown in each of the figures are equally "safe" in the sense that they all have $h = 1.0$ or $h = 1.5$ m, not all are appropriate for the same parent slope. Unless the constant EFH landing surface shape is pre-formed from the base slope, much of the shape of the jump surface will need to be fabricated from snow. Certain of the surfaces will take more snow budget than others, another of the design tradeoffs mentioned above in Sect. 2.3. So the ultimate choice from the family of landing surfaces in Fig. 7 might be the least expensive in terms of snow budget.

Also shown in Fig. 7 are sets of jumper paths, the uppermost of which corresponds to a 26 m horizontal jump distance requiring a design speed of 18.9 m/s. As discussed more completely below, once a constant EFH landing surface that fits the parent slope is chosen, it is essential that the entire portion of it, out to the point of its intersection with the maximum design speed jumper path, be used. Otherwise, some speeds below the maximum design speed will not be accounted for in the design and it will be possible that faster jumpers will be able to over-jump the constant EFH landing region, landing on a portion of the snow where the EFH has not been controlled though surface shape. The design procedure now consists of choosing one of the constant EFH landing surfaces (say from Figs. 7 and 8 or another similar one) to build on the hill.

Thus far the focus has been mostly on the role of only one of the constant EFH landing surface parameters, h. The parameter θ_T can also play an important role in the design in the following way. Figures 7 and 8 contain only four families of constant EFH landing surfaces, but there is a similar infinite set of constant EFH landing surfaces for every other pair of values of takeoff angle θ_T and h. Thus if, after the first try, none of the constant EFH landing surfaces in Figs. 7 and 8 satisfies all the design constraints (e.g. perhaps there is not enough room in the chosen resort location to fit in the complete constant EFH landing surface all the way to the maximum design speed point), then the designer can select from another figure containing constant EFH landing surfaces for the same value of h but for a different takeoff angle, say $h = 1$ and $\theta_T = 13°$ as illustrated below [20].

How does the design of the other components affect the design of the constant EFH landing surface, especially in the light of the fact that these surfaces are velocity-robust? A substantial fraction of the serious SCIs incurred in terrain

park jumps occur as a result of over-jumping the intended landing region. *Thus, perhaps the most critical factor to insure is that over-jumping cannot occur*. The constant EFH landing surfaces discussed here are able to insure that EFH is limited to the design value of h, but only if the entire surface out to the maximum design speed point is employed.

The key connections are the ramp takeoff angle and the design velocity. If the entire constant EFH landing surface were able to be chosen as the design solution, then all takeoff velocities would be accounted for. But often only a finite segment of the constant EFH landing surfaces can fit in the space restrictions in a given location. This implies that only velocities up to a certain takeoff velocity are protected against, in the sense that EFH is limited to h only up to this speed. This "maximum design speed" must be large enough to bound all reasonably possible speeds that can be chosen by the jumper. If this is not the case, then some manner of limiting the takeoff speed must be adopted (such as limiting the start height) so that the constant EFH region of the landing surface cannot be out-jumped.

Terrain park jumps are supposed to be fun. Young athletic skiers and snowboarders jump because it is exhilarating. The exhilaration stems from two main factors: *flight time* during which tricks and other maneuvers can be performed, and *air height*, defined as the maximum vertical distance between the jumper path and the landing surface at any point along the path. An essential tradeoff in the design is between safety and exhilaration. Finding the right balance is the key: designing in an appropriate amount of exhilaration while maintaining the maximum amount of safety possible.

A previous study by Hubbard [20] has shown that constant EFH landing jumps can still provide the flight time and jump air height to be considered "fun". To a good approximation, given a takeoff angle and EFH, both flight time and air height increase roughly linearly as the distance jumped increases, and this is nearly independent of the particular member of the infinite surface family chosen for that takeoff angle and EFH [20]. Considerable exhilaration can be achieved while maintaining adequate safety since, for example, when $h = 1.0$ m, and $\theta_T = 30°$, a flight time and air height of roughly 2 s and 3 m, respectively, can be achieved on jumps about 30 m long.

Consider briefly the issue of rider variability. Perhaps the most common rider variable is the so-called "pop", or jump just before takeoff. This phenomenon can be treated in design by altering the initial conditions as described in Eq. 12 and was indirectly examined experimentally by Shealy et al. [32] who provided the raw data used by McNeil [31] to extract "pop" speeds for over 240 jumpers. McNeil found that for the larger jump studied by Shealy, et al. [32], the maximum positive "pop" speed added was about 1.2 m/s. Figure 9 shows one of the constant EFH surfaces along with several trajectories of jumpers who have "popped" the takeoff. Of course, the EFH for the constant EFH surface is only constant if the rider leaves the takeoff at the same angle as that of the takeoff ramp. Since adding "pop" alters the takeoff angle, the EFH for the resulting landings will be different. One sees that by using a constant EFH surface designed for $h = 1.0$ m and $\theta_T = 25°$, the maximum EFH experienced by the rider adding 1.2 m/s of positive "pop" is 1.44 m. This is still within the USTPC maximum EFH criterion of 1.5 m. In other words all trajectories on this surface with or without "pop" over the entire range of "pop" speeds measured in the field will satisfy the USTPC criterion of EHF below 1.5 m. Also shown in Fig. 9 is the jumper trajectory including both positive "pop" and drag (using the same parameters used in Sect. 2). Note that the two effects nearly cancel resulting in a trajectory very close to the original (no drag and no "pop") case.

5.1 Example of the jump design process using modelling

As an illustration of the iterative design process, several example designs are shown that employ some of the concepts discussed above and illustrate some of the design tradeoffs. Any such design begins with a vertical section of the parent slope. For simplicity and to illustrate the principles, first assume that the parent slope consists of a constant slope equal to the approach angle, $\theta_P = \theta_A = 15°$. Generalization to any slope profile is straightforward. The design question is then: Which candidate constant EFH surface to choose and where and how to place it on the parent slope?

The first important consideration is that to turn the velocity vector, from basically "down" during the approach to "up" at takeoff, requires space and, if the chosen surface is not pre-formed from earth, also requires a considerable investment in snow. The approach, transition, and takeoff are the same for the standard tabletop and the constant EFH jump. As can be seen from Fig. 1, the transition requirement pushes the takeoff, maneuver and landing areas outward away from the parent slope. Table 2 lists the vertical distance from the parent slope to the lip of the takeoff $(y_{lip} - y_{parent})$, for sets of approach parameters, all assuming an approach angle $\theta_A = 15°$. In general, the larger the transition radius and takeoff angle, the more space is required. Thus, the takeoff point needs to be positioned significantly above the parent slope as shown in Fig. 10.

To prevent the landing surface from being over-jumped, the jumper path corresponding to the highest speed attainable (the *maximum design speed*) must intersect a chosen constant EFH landing surface. Further, this surface

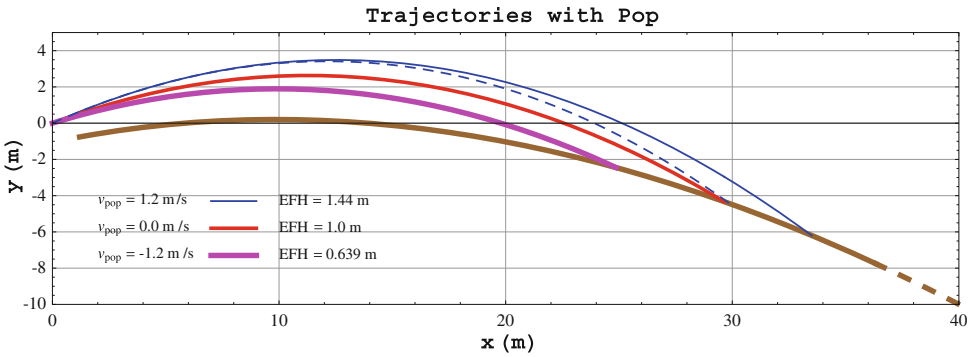

Fig. 9 Large jump trajectories including rider "pop" landing on a constant EFH landing surfaces for $h = 1.0$, $\theta_T = 25°$, and the boundary condition set at $\{x_F = 40\ \text{m}, y_L(x_F) = -10\,\text{m}\}$. The "pop" speeds shown are $v_p = \{-1.2, 0.0, +1.2\}$ m/s resulting in EFHs of {0.639, 1.00, 1.44} m, respectively. In other words all trajectories on this surface with or without "pop" will satisfy the USTPC criterion of EHF below 1.5 m. Also shown is the $v_p = +1.2$ m/s jumper trajectory including drag/lift (*dashed*). Note that the drag effect in this case nearly cancels the effect on range from the positive "pop"

Table 2 Height of takeoff above parent slope

Takeoff angle θ_T (°)	Curvature radius of transition R (m)	Height of takeoff $(y_{lip} - y_{parent})$ (m)
10	15	3.205
25	15	6.295
10	20	3.690
25	20	7.506

must be able to be built in practice. In other words, this path must intersect the chosen landing surface above the practical buildable limit $\theta_L \leq 30°$. Any landing surfaces lying below, and not intersecting the maximum design speed path, do not protect the jumper at all speeds up to the maximum design speed.

If it is not possible, due either to lack of space or inadequate snow budget, to select a landing surface that protects at the maximum design speed, it will be essential to limit the maximum takeoff speed by limiting the length of the approach as described in Sect. 2. Thus this most important design consideration that *the landing surface not be able to be over-jumped* should be primary.

To be specific, consider the situation shown in Fig. 10a, b showing a parent slope with angle $\theta_P = 15°$ and ten candidate constant EFH surfaces, all with $h = 1.0$ m and for $\theta_T = 10°$ and $\theta_T = 25°$, respectively. The jumper path corresponding to the maximum design speed is based on an approach length of 100 m for the low friction case. From Fig. 2 this gives $v \simeq 15.0$ m/s $= 33.6$ mph. In Fig. 10a the maximum speed jumper path intersects five of the ten candidate surfaces shown and therefore only these (highest) five candidates protect the jumper at all speeds up to the maximum design speed. The lowest of these candidates is the cheapest from a snow budget point of view, since less snow needs to be added to the parent slope to support the shape of the surface. This gives a general design rule of thumb: *the most economical constant EFH surface to build is the one that intersects the jumper maximum design speed path at the buildability limit or at the parent slope*.

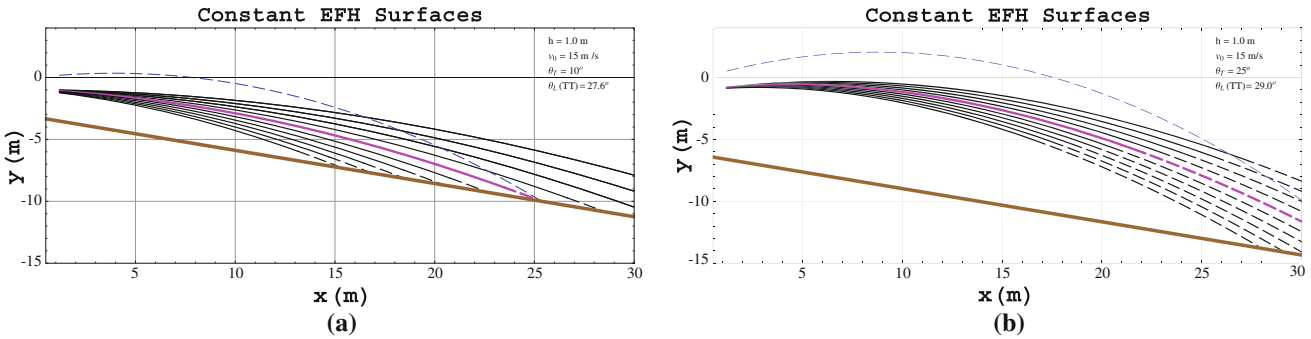

Fig. 10 The parent slope (*brown*) and ten constant EFH landing surfaces for $h = 1.0$ for **a** $\theta_T = 10°$ and **b** $\theta_T = 25°$. Also shown are the jumper paths (*dashed*) corresponding to the horizontal jump distance at the maximum design speed for an approach length of 100 m (15 m/s). The constant EFH surface that intersects the parent slope at this point is thicker (*magenta*). The buildable limit $\theta_L = 30°$ on the constant EFH surfaces is identified by transition to a *dashed line* beyond which fabrication is impractical with present snow grooming equipment without use of a winch (colour figure online)

Having chosen a landing surface that intersects the maximum design speed jumper path, one defines the *jump length* x_L as the value of x where this intersection occurs. The artificially constructed landing surface (for $x < x_L$) must thereafter rejoin the parent slope(for $x > x_L$) but since, by definition, there can be no landings in this region, there is more flexibility in its shape. Although a mathematical expression could be used to characterize the surface this is not essential. One simply assumes that this *bucket* region is a smooth transition that limits surface curvature, and thus normal acceleration, to reasonable values.

Occasionally there may be restrictions on the space available for placement of the jump. For example, these might be expressed as $0 < x < x_S$ and $y(0) < y < y(x_S)$, the interior of a rectangle inside which the jump landing surface must lie. In such a case the intersection of the maximum design speed path with a constant EFH surface for the specified value of h and chosen value of θ_T may not exist within the rectangle, i.e. it may not be possible to build a landing surface that limits EFH to h over a reasonable set of takeoff speeds with the given takeoff angle.

As an example, having chosen $\theta_T = 25°$ and $h = 1.0$ m, suppose it is desired to restrict space to $x < x_S = 20$ m. It is clear from Fig. 10b that none of the constant EFH landing surfaces intersect the maximum design speed jumper path within this region, and thus none of these will protect at the $h = 1.0$ m level for the value of $\theta_T = 25°$. Then, either the maximum design speed must be changed by limiting takeoff velocity by restricting the approach length, or another constant EFH surface must be chosen above the ten shown, or the takeoff angle must be modified. This last choice as a design option corresponds to using, say, Fig. 10a as the design template instead, in which there is one of the constant EFH surfaces that meets both the space and the maximum design speed constraints.

A general design rule of thumb arises from this example: *it is always possible, by decreasing the takeoff angle, to choose a constant EFH surface lying within any restricted region that limits h to a given value*. This shows that all three of the design variables, θ_T, h, and the particular surface chosen from the infinite family are important.

Figure 11a shows an example constant EFH surface choice replacing an example tabletop surface (parameters are given in the caption) along with sample trajectories for a takeoff angle of $\theta_T = 13°$. In this example, at $x \sim 23$ m the constant EFH surface reaches the practical slope angle limit of 30°. To be realistic, at this point the constant EFH surface (solid) transitions to a constant slope (dashed) surface with constant $\theta_L = 30°$ until it intersects the parent surface.

Figure 11b shows the resulting EFHs for the tabletop and constant EFH landing surfaces. Since this constant EFH landing surface was calculated assuming no drag, it yields a value $h = 1$ m for jumper paths without drag. By design, the constant EFH landing surface provides a constant 1.0 m EFH out to $\sim$23 m at which, as discussed previously, the landing angle is a constant 30°, so the EFH rises linearly as expected for a straight landing surface but still only exceeds the USTPC criterion value of 1.5 m after $x \simeq 27$ m, the maximum design jump distance and an unusually long jump of over 27 m. The standard tabletop surface exceeds the USTPC criterion for the entire length of the deck before dropping briefly to acceptable values between $9.1\,\text{m} < x < 22$ m. For $x > 22$ m the EFH for the tabletop rises approximately linearly to a value of about 2.4 m at $x = 30$ m. Clearly the constant EFH surface provides greater protection for the two hazardous situations of landing short (on the deck) and landing "deep". If holding the EFH to the USTPC criterion is deemed important enough, perhaps it would be worth using a winch to increase the angle of the constant EFH surface in the relatively small 7 m long region $22.6 < x < 30$ m Also shown in Fig. 11b is the small added effect of including drag on the EFH for the constant EFH surface (dashed line). Since this constant EFH landing surface was calculated assuming no drag, it yields a value $h = 1$ m for jumper paths without drag. The effect of drag on the resulting EFH for this jump is modest.

Even though the straight tabletop landing surface enjoys a lower EFH for part of the landing surface, the constant EFH landing surface in Fig. 11a obviously protects the jumper more effectively over a greater range of jump distances. Furthermore, the cost of the added protection in terms of snow budget is quite small. The volume of snow per unit width of the landing surface in these examples is 72.3 m^2 for the tabletop and 76.2 m^2 for the constant EFH surface. Designers will need to include this economic fact in their considerations. If snow budget becomes an unmanageable constraint, an alternative approach is to preform the hill to lower the snow required, but this option removes some flexibility in moving or significantly altering jump shapes in mid-season and probably incurs significantly more earthmoving expense.

For the reasons explained above, building a jump entirely above a constant slope can be expensive. Terrain park personnel figured out long ago that taking advantage of natural undulations in the parent surface can minimize this expense. Essentially the jump is put at a location on the parent slope that uses the natural topography rather than snow to fill in the volume below the landing surface. This strategy is effective with constant EFH landing surfaces as well for tabletops.

Nevertheless, it may sometimes be desired to place a jump on a constant slope. If the terrain is malleable (not bedrock) the rough jump shape may be sculpted from the

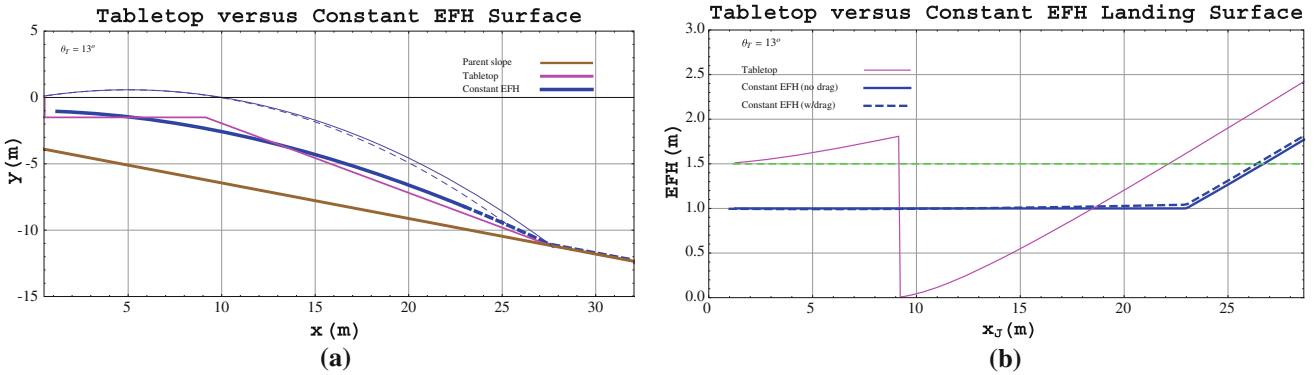

Fig. 11 **a** Comparison of an example standard tabletop (*magenta*) and constant EFH (*blue*) landing surfaces along with example jumper trajectories for $\theta_T = 13°$. The landing surfaces end at the run-out when intersecting with the parent slope (*brown*) at $x \simeq 27$ m. **b** Comparison of the EFH values for the standard tabletop and constant EFH landing surfaces. The tabletop has a lip height of 1.5 m, a deck length of 30 ft, and a landing slope angle of 27.6° chosen to intersect the parent surface at the maximum jumper path for the design speed (15.0 m/s) based on an approach length of 100 m. The constant EFH surface has $h = 1.0$ m and continues until $x \simeq 23$ m at which point the landing angle equals 30°. Beyond this point the landing angle is constant at $\theta_L = 30°$ (*dashed line*) until it intersects the parent slope. The *horizontal dashed* (*green*) *line* in **b** marks the EFH = 1.5 m USTPC criterion value (colour figure online)

earth by excavation rather than from snow each season. The shape of the landing surface is formed from earth rather than snow and thus need not require large amounts of expensive artificial snow. An example of such topographical preforming would have the approach partially submerged below the original parent surface, and the earth from this cut would then be pushed downhill to form the takeoff ramp and part of the landing surface. After the snow is added, the entire jump would conform much more closely to the parent slope, being sometimes above and sometimes below the original parent slope, saving considerably on the snow required to fine tune the shape and provide enough base to ensure the parent slope is unlikely to ever be exposed. This permanent fabrication of the jump shape will likely be more expensive initially, but it would require less additional snow and shaping each snow season thereafter, and may be the most economical design option especially in a region with limited natural snow and artificial snow budgets. Whether this is an economically feasible option will depend on the details of the terrain park jump location, base parent slope, annual snowfall and snow making ability, grooming equipment and maintenance resources, and crucially on the energy cost of artificial snow.

6 Summary

Winter terrain park jumps have been shown to present a special hazard to ski resort patrons for spine, neck, and head injuries. Presently, such jumps are built without a quantitative engineering design approach based on the assertion by the NSAA and supported by some researchers that there is too much variation in the conditions and rider decisions. However, recent studies by the authors and others have examined these factors and determined that while they do indeed vary, they do so in an understandable and bounded fashion that can be accommodated or rendered irrelevant by the design. The role of modelling the behaviour of a jumper executing a terrain park jump enables and informs an intelligent design process that meets reasonable performance criteria while satisfying the constraints of the parent terrain, snow budget, and safety considerations. The paper concluded with an illustrative example of the design of a constant EFH jump on a hypothetical terrain park parent slope. It was shown that, unlike the tabletop design, an appropriately designed constant EFH landing surface can satisfy the USTPC criterion for maximum EFH for all values of the takeoff speed including rider "pop" effects. These insights were made possible by the extensive use of computer modelling in setting up, constraining, and solving for the relevant design parameters.

There are several ways in which the present work may be extended and improved. Many of the physical parameters such as the range of drag and friction coefficients were estimated from older published research of a generic nature and better values appropriate to actual snowboarders and skiers are needed. Once these physical parameters are better determined, on-slope validation of the trajectory and rigid body models would improve general acceptance of this approach as well as lead to further insights to improve the model. Finally, the modelling of trajectories is only part of the story. Better modelling of the human factors related to the range of rider actions prior to the takeoff, in the air, and upon landing would greatly improve our understanding of how riders interact with winter terrain park jumps.

Acknowledgments The authors acknowledge useful discussions with and helpful suggestions from J. Brodie McNeil, A.Wisniewski, and a terrain park manager who requested anonymity.

References

1. Tarazi F, Dvorak MFS, Wing PC (1999) Spinal injuries in skiers and snowboarders. Am J Sports Med 27:2
2. Moffat C, McIntosh S, Bringhurst J, Danenhauer K, Gilmore N, Hopkins CL (2009) Terrain park injuries. West J Emerg Med 10:4
3. Russell K (2011) The relationship between injuries and terrain park feature use among snowboarders in Alberta (thesis). University of Calgary, Calgary, Canada
4. Henrie M, Petron D, Chen Q, Powell A, Shaskey D, Willick S (2011) Comparison of ski and snowboard injuries that occur inside versus outside terrain parks. Presented at the international society for safety in skiing 19th international congress on ski trauma and safety. Keystone, Colorado. Abstract published in the book of abstracts of the 19th international congress on ski trauma and skiing safety
5. National Ski Areas Association. http://www.nsaa.org/nsaa/press/facts-ski-snbd-safety.asp. Accessed Sept 2011
6. Shealy JE, Scher I, Johnson RJ (2012) Jumping features at ski resorts: good risk management or not? In: Skiing trauma and safety (ASTM STP 1553), vol 19. ASTM, West Conshohocken (forthcoming)
7. Sutherland AG, Holmes JD, Meyers S (1996) Differing injury patterns in snowboarding and alpine skiing. Injury 27(6):423–425
8. Dohjima T, Sumi Y, Ohno T, Sumi H, Shimizu K (2001) The dangers of snowboarding: a 9-year prospective comparison of snowboarding and skiing injuries. Acta Orthop Scand 72(6):657–660
9. Shealy JE, Ettlinger CF, Johnson RJ (2000) Rates and modalities of death in the U.S.: snowboarding and skiing differences 1991/92 through 1998/99. In: Johnson RJ, Zucco P, Shealy JE (eds) ASTM STP 1397, skiing trauma and safety, vol 13. ASTM, West Conshohocken, pp 132–138
10. Greve MW, Young DJ, Goss AL, Degutis LC (2009) Skiing and snowboarding head injuries in 2 areas of the United States. Wilderness Environ Med 20:234–238
11. Meyers AR, Misra B (1999) Alpine skiing and spinal cord injuries: view from a national database. In: Skiing trauma and safety (ASTM STP 1345), vol 12. ASTM, West Conshohocken, pp 150–157
12. Jackson AB, Dijkers M, DeVivo MJ, Poczatek RB (2004) A demographic profile of new traumatic spinal cord injuries. Arch Phys Med Rehabil 85:1740–1748
13. Ackery A, Hagel BE, Provvidenza C, Tator CH (2007) An international review of head and spinal cord injuries in alpine skiing and snowboarding. Injury Prev 13:368–375
14. Seino H, Kawaguchi S, Sekine M, Murakami T, Yamashita T (2001) Traumatic paraplegia in snowboarders. Spine 26(11): 1294–1297
15. DeVivo M, Whiteneck G, Charles E (1995) The economic impact of spinal cord injury. In: Stover S, DeLisa J, Whiteneck G (eds) Spinal cord injury: clinical outcomes from the model systems. Aspen Publishers, Gaithersburg, pp 234–271
16. Dijkers M, Abela M, Gans B, Gordon W (1995) The aftermath of spinal cord injury. In: Stover S, DeLisa J, Whiteneck G (eds) Spinal cord injury: clinical outcomes from the model systems. Aspen Publishers, Gaithersburg, pp 185–212
17. Ski Area Management. http://www.saminfo.com/. Accessed Sept 2011
18. National Ski Areas Association (2008) Freestyle Terrain Park Notebook
19. Bohm H, Senner V (2009) Safety in big jumps: relationship between landing shape and impact energy determined by computer simulation. In: Johnson RJ, Shealy JE, Langren M (eds) Skiing trauma and safety (ASTM STP 1510), vol 17. ASTM International, West Conshohocken
20. Hubbard M (2009) Safer ski jump landing surface design limits normal velocity at impact. In: Johnson RJ, Shealy JE, Langren M (eds) Skiing trauma and safety (ASTM STP 1510), vol 17. ASTM International, West Conshohocken
21. McNeil JA, McNeil JB (2009) Dynamical analysis of winter terrain park jumps. Sports Eng 11(3):159–164
22. Swedberg A (2010) Safer ski jumps: design of landing surfaces and clothoidal in-run transitions (thesis). Naval Postgraduate School, Monterey
23. Streeter VL, Wylie EB, Bedford KW (1998) Fluid mechanics, 9th edn. McGraw-Hill, Boston, pp 332–339
24. Hoerner SF (1965) Fluid dynamic drag. SF Hoerner, Bakersfield (Lib. of Congress Card No. 64-19666)
25. Kittel C, Kroemer H (1980) Thermal physics, 2nd edn. W. H. Freeman, San Francisco
26. Lind D, Sanders S (2003) The physics of skiing, 2nd edn. Springer, New York, p 179
27. Colbeck SC (1992) CRREL monograph 92-2: a review of the processes that control snow friction. U.S. Army Corps of Engineers, Cold Regions Research and Engineering Laboratory, Hanover
28. US Terrain Park Council. http://usterrainparkcouncil.org. Accessed Sept 2011
29. Swedberg A, Hubbard M (2012) Models of table-top jump geometry show they may not limit equivalent fall height. In: Skiing trauma and safety (ASTM STP 1553), vol 19. ASTM, West Conshohocken (forthcoming)
30. Hubbard M, Swedberg A (2012) Jump landing surface design for constant equivalent fall height is robust to 'uncontrollable' factors. In: Skiing trauma and safety (ASTM STP 1553), vol 19. ASTM, West Conshohocken (forthcoming)
31. McNeil JA (2012) Modelling the 'Pop' in winter terrain park jumps. In: Skiing trauma and safety (ASTM STP 1553), vol 19. ASTM, West Conshohocken (forthcoming)
32. Shealy JE, Scher I, Stepan L, Harley E (2010) Jumper kinematics on terrain park jumps: relationship between takeoff speed and distance traveled. J ASTM Int 17(10):1. doi:10.1520/JAI102885
33. McNeil JA (2012) The inverting effect of curvature on winter terrain park jump takeoffs. In: Skiing trauma and safety (ASTM STP 1553), vol 19. ASTM, West Conshohocken (forthcoming)
34. Shealy JE, Stone F (2008) Tabletop jumping: engineering analysis of trajectory and landing impact. J ASTM Int 5(6):1
35. McNeil JA (2012) Discussion on 'Tabletop jumping: engineering analysis of trajectory and landing impact' by Shealy and stone. In: Skiing trauma and safety (ASTM STP 1553), vol 19. ASTM, West Conshohocken (forthcoming)